DOI: 10.1002/chem.200701803

# Luminescent Excited-State Intramolecular Proton-Transfer (ESIPT) Dyes Based on 4-Alkyne-Functionalized [2,2′-Bipyridine]-3,3′-diol Dyes

**Gilles Ulrich,*[a] Francesco Nastasi,[b] Pascal Retailleau,[c] Fausto Puntoriero,[b] Raymond Ziessel,*[a] and Sebastiano Campagna*[b]**

**Abstract:** Functionalized 6,6′-dimethyl-3,3′-dihydroxy-2,2′-bipyridine dyes ($BP(OH)_2$) exhibit relatively intense fluorescence from the relaxed excited state formed by excited-state intramolecular proton transfer (ESIPT). Bromo functionalization of ($BP(OH)_2$) species followed by palladium(0)-catalyzed reactions allows the connection (via alkyne tethers) of functional groups, such as the singlet-emitter diazaboraindacene (bodipy) group or a chelating module (terpyridine; terpy). The X-ray structure of the terpy-based compound confirms the planarity of the 3,3′-dihydroxy-bipyridine unit. The new dyes exhibit relatively intense emission on the nanosecond timescale when in fluid solution, in the solid state at 298 K, and in rigid glasses at 77 K. In some cases, the excitation wavelength luminescence was observed and attributed to 1) inefficiency of the ESIPT process in particular compounds when not enough vibrational energy is introduced in the Franck–Condon state, which is populated by direct light excitation or 2) the presence of an additional excited state that deactivates to the ground state without undergoing the ESIPT process. For some selected species, the effect of the addition of zinc salts on the absorption and luminescence spectra was investigated. In particular, significant fluorescence changes were observed as a consequence of probable consecutive formation of a 1:1 and 1:2 molecular ratio of ligand/zinc adducts owing to coordination of $Zn^{II}$ ions by the bipyridyldiol moieties, except when an additional terpyridine subunit is present. In fact, this latter species preferentially coordinates to the $Zn^{II}$ ion in a 1:1 molecular ratio and further inhibits $Zn^{II}$ interaction. In the hybrid Bodipy/$BP(OH)_2$ species, complete energy transfer from the $BP(OH)_2$ to the bodipy fluorophore occurs, leading to exclusive emission from the lowest-lying bodipy subunit.

**Keywords:** alkynes · excited states · fluorescence · luminescence · Zn complexes

## Introduction

The search for new, efficient fluorescent molecules has attracted the attention of scientists in the last decade owing to their potential application in medicinal diagnostic, biological labeling, molecular detection, and optoelectronic materials.[1] Most of the organic fluorescent systems are based on singlet excited-state emission, some on triplet emission, and a few on the luminescence properties of excited-state proton-transfer species. The latter species exhibit interesting features such as large Stokes'shift compared with singlet emitters, while retaining relatively high quantum yields. The well known coumarin family members (including some commercial Alexa dyes[2]) are a typical examples of this fluorescence mechanism in which the proton transfer takes place between the solvent and the solute. Nevertheless, this photochemically generated fluorescent solution leads to intrinsic chemical instability. The use of molecular systems with intramolecular excited-state proton-transfer abilities could offer higher stability. From the examples found in the literature, such as salicylates,[3] *O*-hydroxyphenyl pyridine,[4] or *O*-hydroxyphenyl benzothiazole,[5] we focused our attention on functionalized 2,2′-bipyridyl-3,3′-diols.[6] This choice was mo-

[a] Dr. G. Ulrich, Dr. R. Ziessel
Laboratoire de Chimie Moléculaire, École de Chimie, Polymères, Matériaux (ECPM)
Université Louis Pasteur (ULP)
25 rue Becquerel, 67087 Strasbourg Cedex 02 (France)
E-mail: gulrich@chimie.u-strasbg.fr
ziessel@chimie.u-strasbg.fr

[b] F. Nastasi, F. Puntoriero, S. Campagna
Dipartimento di Chimica Inorganica, Chimica Analitica e Chimica Fisica
Università di Messina
via Sperone 31, 98166, Messina (Italy)
E-mail: campagna@unime.it

[c] P. Retailleau
Laboratoire de Cristallochimie, ICSN - CNRS
Bât 27–1 avenue de la Terrasse, 91198 Gif-sur-Yvette, Cedex (France)

   

tivated by the good luminescence properties and the possible chemical functionalization of the units,[7] which allows connection of a chelating subunit for detection purposes[8] or of a second dye to build an energetic cascade.[9]

Bipyridyldiol species (henceforth abbreviated as $BP(OH)_2$) are extensively studied for both theoretical and applicative reasons.[10] $BP(OH)_2$ compounds are ideal systems to investigate excited-state intramolecular proton transfer (ESIPT) processes: indeed, upon excitation (Figure 1**;** a), the O−H bond strength is reduced and the protons, already hydrogen-bonded to the nitrogen atoms of the pyridyl rings in the ground state, are totally transferred to the pyridine nitrogen atoms. This process can take place on the singlet excited-state adiabatic hypersurface (Figure 1**;** b) and is ultrafast, typically in the picosecond timescale.[11] The minimum on the excited-state potential-energy surface corresponds therefore to the ground state proton-transfer tautomer. The relaxed excited state deactivates by radiative (and radiationless) transitions (Figure 1**;** c) followed by back proton transfer onto the ground-state hypersurface, which regenerates the initial species (Figure 1; d). The various processes can be influenced by solvents and substituents on the bipyridyl rings.[7a] From the viewpoint of potential applications, the title species is of interest for the luminescence properties of their relaxed excited states, which make them appealing as sensors and for the design of three-level laser systems.[12]

Herein we report the synthesis, characterization, absorption spectra, and photophysical properties (both at room temperature in acetonitrile solution and at 77 K in EtOH/MeOH 4:1 v/v rigid matrix) of five new $BP(OH)_2$ molecules, **2**–**6**. The structural formulas of the new species are shown in Scheme 1. Most of the new species contain substituents that should allow them to connect to other photo- or redox-active subunits and/or additional chromophores. Therefore, **2**–**6** can also be regarded as part of a library for the development of multicomponent photoactive species.

**Abstract in French:** *Des composés colorés à base de 6,6′-dimethyl-3,3′-dihydroxy-2,2′-bipyridine ($BP(OH)_2$) ont été synthétisés et présentent une fluorescence relativement intense issue de la relaxation d'un état excité provenant d'un transfert de proton dans l'état excité (ESIPT). La bromation de dérivés ($BP(OH)_2$) suivie d'un couplage croisé catalysé par du $Pd^0$ sous-ligandé permet de connecter (par l'intermédiaire de pont alcyne) des groupes fonctionnels comme un groupe émetteur singulet de type boradiazaindacène (Bodipy) ou un module chélatant universel (une terpyridine). Une structure par diffraction aux rayons X a été obtenu avec le dérivé terpyridine, celle ci confirme la planéité de l'unité 3,3′-dihydroxy-bipyridine. Les nouveaux fluorophores possèdent une émission relativement intense avec une durée de vie de l'ordre de la nanoseconde, en solution et à l'état solide à 298 K ainsi que dans un verre à 77 K. Dans certain cas, la luminescence dépend de la longueur d'onde d'excitation, ce phénomène est attribué à (i) l'inefficacité du processus ESIPT, quand trop peu d'énergie vibrationnelle est introduite dans l'état Franck-Condon peuplé directement par la lumière d'excitation (ii) la présence d'un état excité supplémentaire qui désactive l'état fondamental sans passer par un processus ESIPT. Pour certains composés, l'effet de l'addition de sels de Zinc sur les spectres d'absorption et d'émission a été étudié : en particulier, des changements significatifs de fluorescence ont été observés, probablement due à la formation consécutive de complexes ligand/zinc de stœchiométrie 1:1 et 1:2, provenant de la coordination des cations $Zn^{II}$ par l'unité bipyridyl-diol, sauf quand une fonction terpyridine est présente. En fait, dans cette dernière espèce le zinc est préférentiellement coordiné par la terpyridine dans un ratio 1:1, et toute coordination supplémentaire de Zinc semble inhibée. Dans le composé hybride Bodipy/$BP(OH)_2$, un transfert d'énergie quantitatif est observé du $BP(OH)_2$ vers le fluorophore Bodipy, entraînant une émission exclusive de la sous-unité Bodipy.*

**Abstract in Italian:** *Composti basati sulla subunità 6,6′-dimetil-3,3′-dididrossi-2,2′-bipiridina ($BP(OH)_2$), variamente funzionalizzati, presentano fluorescenza relativamente intensa da stati eccitati formati attraverso trasferimento protonico nello stato eccitato (ESIPT). Bromo-funzionalizzazione dei composti di tipo $BP(OH)_2$, seguita da reazioni catalizzate da Pd(0), permettono di connettere (con legame alchinico) gruppi funzionali quali il diazaboroindacene (Bodipy) o un modulo chelante (terpiridina) al frammento $BP(OH)_2$. La struttura ai raggi X del composto contenente la terpiridina conferma la planarità dell'unità 3,3′-diidrossi-bipiridina. Le nuove specie presentano intensa emissione nella scala dei nanosecondi, in soluzione fluida ed allo stato solido a 298 K ed in matrice rigida a 77 K. In alcuni casi, la luminescenza dipende dalla lunghezza d'onda di eccitazione: questo fenomeno è attribuito a (i) inefficienza del processo ESIPT, quando non sufficiente energia vibrazionale è introdotta nello stato Franck-Condon a seguito di eccitazione luminosa o (ii) alla presenza di uno stato eccitato addizionale che si disattiva allo stato fondamentale senza passare dallo stato eccitato prodotto attraverso il meccanismo ESIPT. Per composti selezionati è stato anche studiato l'effetto della presenza di sali di zinco sulle proprietà di assorbimento elettronico e di luminescenza: significativi cambiamenti della fluorescenza sono stati osservati, come conseguenza della consecutiva formazione di addotti 1:1 e 1:2 (rapporto molare $BP(OH)_2$/zinco), dovuta alla coordinazione di cationi di $Zn^{II}$ da parte del bipiridil-diolo, che si verifica in tutti i casi studiati tranne in presenza di una subunità terpiridinica. In quest'ultimo caso, infatti, si forma soltanto l'addotto 1:1, e ulteriore coordinazione di cationi di $Zn^{II}$ appare inibita. Nella specie ibrida Bodipy/$BP(OH)_2$ si verifica un completo trasferimento di energia elettronica dal $BP(OH)_2$ al Bodipy, che porta ad emissione esclusivamente dalla subunità Bodipy, a piû bassa energia.*

  

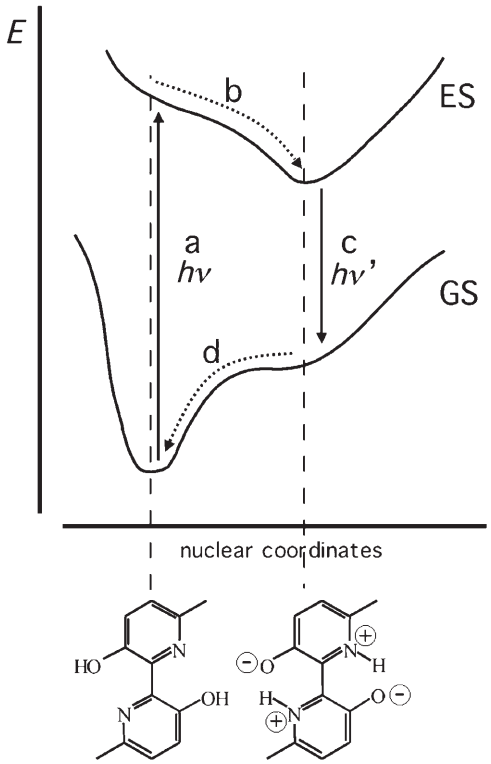


Figure 1. Pictorial representation of the potential-energy hypersurfaces of the ground (GS) and excited (ES) states of bipyridyldiol compounds and of the related processes. Schematic structures corresponding to the ground- and excited-state minima are also shown.

Notably, there has been some debate as to whether in the $BP(OH)_2$ species two proton transfers occurred in a concerted way or by consecutive processes[13] with formation of an intermediate. Recent investigations definitely indicate that both the mechanisms can operate simultaneously,[13,14] with the concerted one-step, two-proton-transfer mechanism taking place within 50 fs and the consecutive two-step process operating in the tens of fs regime for the first proton transfer and in about 10 ps for the second proton transfer.[13,14] In any case, assistance of vibrational modes seems to be required: in particular, stretching and bending modes are considered to promote the one- and two-step double-proton transfer reactions, respectively.

Here, the mechanistic details of the ESIPT process are not investigated in detail as our investigation mainly deals with the excited-state properties (namely luminescence) of the relaxed excited-state species and as we report on the photophysical properties in the nanosecond timescale, when the ultrafast proton-transfer processes have already occurred.

## Results and Discussion

**Synthesis**: The strongly yellow luminescent starting compound **1** was regioselectively monobrominated by using *N*-bromosuccinimide (NBS) in a *N*,*N*-dimethylformamide (DMF)/dichloromethane mixture, in good yields and at room temperature. Similar bromination reactions were previously performed on 3-hydroxypyridines.[15] A Sonogashira cross-coupling reaction of **2** with trimethylsilylacetylene allowed us to obtain **3** in good yields (Scheme 2) despite the presence of free hydroxy groups. The silyl protective group was readily removed by the action of fluoride salt to give **4**. This active acetylenic group was then coupled via a cross-coupling reaction in the presence of a catalytic amount of $Pd^0$ to a halogeno aromatic compound. As prototypical examples of bright molecular subunits that give a second function to the final molecule, we choose to introduce a universal chelating group: a terpyridyl group (terpy); and a very efficient singlet emitter fluorophore: a boron-dipyrromethene (bodipy) group. By connecting these secondary functions to the $BP(OH)_2$ group, we could induce perturbation of luminescence in the presence of specific analytes and create a dual dye in which energy-transfer processes could be studied.

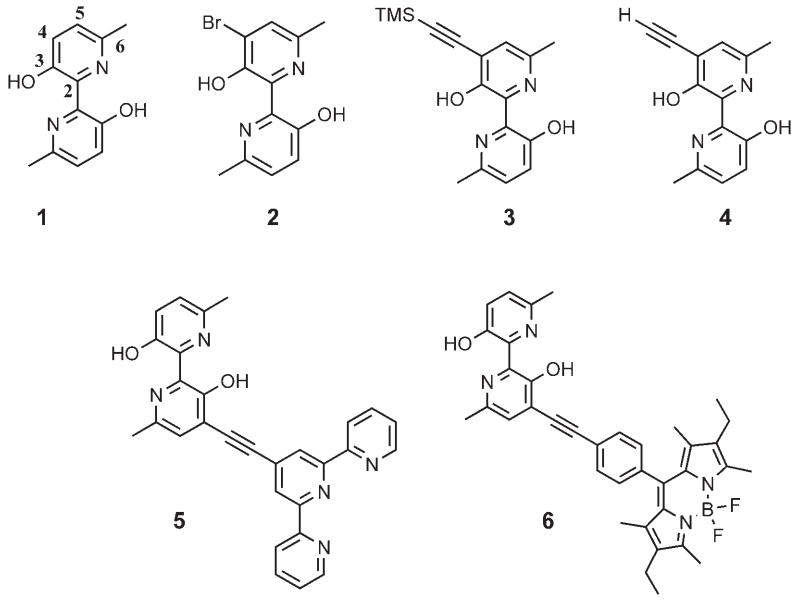


Scheme 1. Structural formulas of the compounds studied.

Compound **4** was thus connected in good yields to 4′-trifluorosulfonato-2,2′:6′,2″-terpyridine or iodophenyl-bodipy[16] by a Sonogashira-type reaction to give **5** and **6,** respectively.

All new compounds were fully characterized by $^1H$ NMR and $^{13}C$ NMR spectroscopy,

  

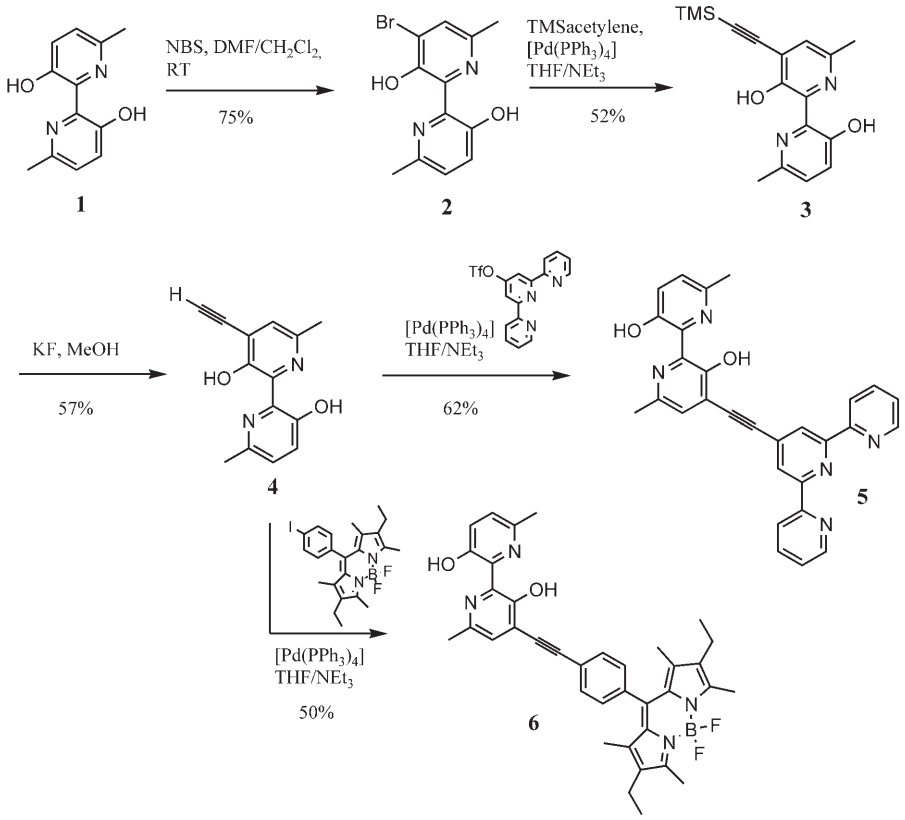


Scheme 2. Synthetic sketch for the preparation of the dyes. TMS = trimethylsilyl.

mass spectrometry, and elemental analysis. In particular, the $^1$H NMR spectra display typical peaks due to the strong intramolecular hydrogen bonds that are observed in the $\delta =$ 14–16 ppm range. The unique singlet at $\delta = 14.7$ ppm, which is observed for **1**, is replaced by two distinct singlets for the dissymetric bipyridine structures **2**–**6**.

**X-ray crystallography**: Single crystals were obtained for compound **5** and used to elucidate the X-ray molecular structure (Figure 2). The molecule crystallized in a monoclinic $P12_11$ space group, with unit-cell dimensions of $a =$ 7.774(2), $b = 32.603(4)$, $c = 10.219(2)$ Å, $\beta = 105.36(0)°$. Two molecules are present in the unit cell with one $CH_2Cl_2$ molecule. The whole molecule **5** is almost planar owing to extended $\pi$ conjugation from the terpyridine group to the $BP(OH)_2$ group through the dangling acetylenic bridge. The terpyridine is in transoid form as is usually observed when it is not coordinated. The $BP(OH)_2$ core is completely planar and in accordance with the crystal structure of **1**.[17] The two molecules in the unit cell present some bond-length variation. As previously observed in the structure of symmetrical 6,6′-dimethyl-3,3′-dihydroxy-2,2′-bipyridine,[17] the C–C and C–O bonds implied in the $BP(OH)_2$ tautomeric equilibrium are about halfway between the accepted values for single and double bond distances (Table 1)

The crystal packing of compound **5** (Figure 3) can be regarded as dimers made of head-to-tail molecule stacks that form waving sheets parallel to

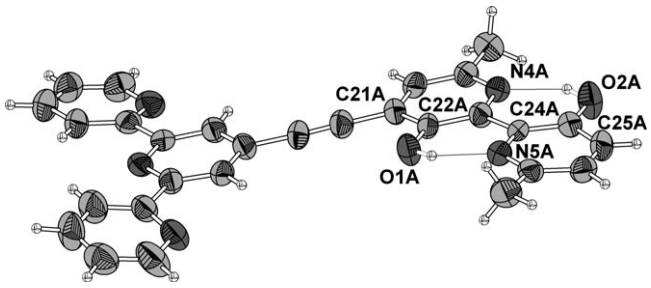


Figure 2. ORTEP plot of the unit cell of molecule **5** (ellipses shown at the 50% probability level). The strong intramolecular hydrogen bonding, reflected by a very short N–O distance of approxiamately 2.57 Å is consistent with the NMR data.

Table 1. Selected bond lengths [Å] of compound **5**.

| | | | |
|---|---|---|---|
| O1A–C22A | 1.342(7) | O1B–C22B | 1.333(7) |
| O2A–C25A | 1.343(8) | O2B–C25B | 1.344(8) |
| N4A–C21A | 1.342(8) | N4B–C21B | 1.338(8) |
| N5A–C24A | 1.351(8) | N5B–C24B | 1.359(8) |
| C21A–C22A | 1.428(9) | C21B–C22B | 1.415(9) |
| C24A–C25A | 1.401(9) | C24B–C25B | 1.388(9) |
| O1A–N5A | 2.535(7) | O1B–N5B | 2.532(7) |
| O2A–N4A | 2.581(7) | O2B–N4B | 2.594(7) |

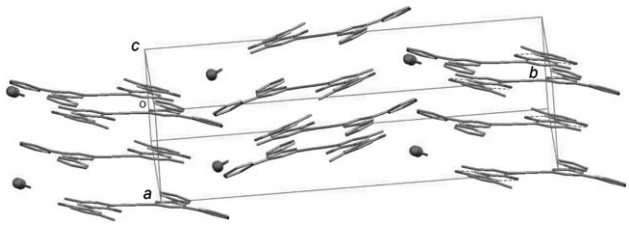


Figure 3. Crystal packing of molecule **5** along the *a* and *c* axis.

(–2 0 2). The distances between the two molecules of the dimer is approximately 3.5–3.6 Å, the shorter distance between the two acetylenic bonds is 3.52 Å. When both acetylenic bonds are coplanar, the bipyridine ring perfectly cover two rings of the terpyridine part. Successive layers of dimer sheets are supported by joint insertion of dichloromethane.

  

The shorter distance between the pile is observed between the non-covered pyridine ring of the terpyridine part, with a 3.7 Å separation.

**Absorption spectra and luminescence properties**: The absorption spectra of **1**–**6** (Table 2, Figure 4) exhibit an intense band between 300 and 450 nm ($\varepsilon$ in the range 10000–25000 $M^{-1}cm^{-1}$), which can be assigned to the spin-allowed $\pi$–$\pi$ transitions involving the hydroxybipyridyl rings. This band is slightly redshifted for **3, 4**, and particularly for **5** in comparison with **1** and **2** because of the presence of the alkynyl substituents. In compound **5**, a strong absorption band with a maximum at 286 nm is also present and is attributed to spin-allowed transitions involving the terpyridine subunit. Compound **6** also exhibits a strong structured absorption in the visible range owing to transitions involving the bodipy dye. The absorption spectra of all the compounds are very similar on passing from acetonitrile to dichloromethane solutions (for example, the lowest-energy absorption maxima of all the dyes are displaced at most by a couple of nanometers), indicating that charge-transfer character is negligible.

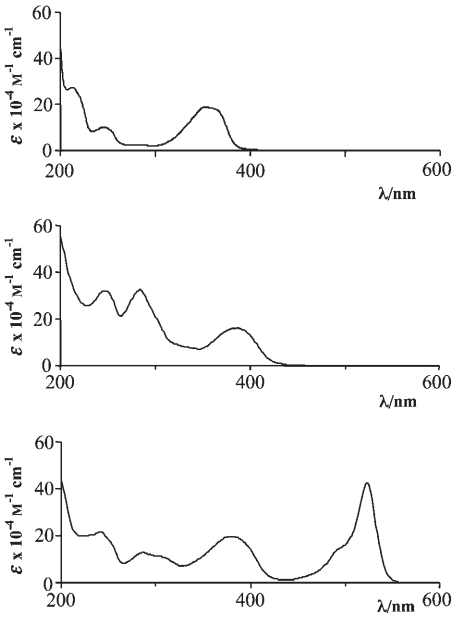


Figure 4. Absorption spectra in acetonitrile of **1** (top), **5** (middle), and **6** (bottom).

Table 2. Absorption and luminescence data for **1**–**6**.[a]

| | Absorption | Luminescence (298 K) | | | Luminescence, solid state (298 K) | | Luminescence (77 K)[b] | |
|---|---|---|---|---|---|---|---|---|
| | $\lambda_{max}$ [nm] ($\varepsilon$ [$M^{-1}cm^{-1}$]) | $\lambda_{max}$ [nm] | $\tau$ [ns] | $\Phi$ | $\lambda_{max}$ [nm] | $\tau$ [ns] | $\lambda_{max}$ [nm] | $\tau$ [ns] |
| **1** | 352 (19100) | 506[d] | 1.1 | 0.1 | 518 | 5.4 | 498 | 5.7 |
| | 246 (10200) | (502)[c] | | | | | | |
| **2** | 356 (17900) | 505[d] | 1.8 | 0.33 | 521 | 4.3 | 500 | 4.8 |
| | 250 sh | (502)[c] | | | | | | |
| **3** | 378 (22400) | 537[e] | 6.4 | 0.013 | 555 | 2.8 | 545 | 2.5 |
| | 238 (28000) | (532)[c] | | | | | | |
| **4** | 370 (20200) | 532[f] | 6.3 | 0.009 | 543 | 1.7 | 535 | 2.8 |
| | 274 (95700) | (530)[c] | | | | | | |
| **5** | 387 (15500) | 571 | 0.4 | 0.005 | 585 | 1.1 | 572 | 1.0 |
| | 284 (31900) | (566)[c] | | | | | | |
| | 247 (29000) | | | | | | | |
| **6** | 525 (42100) | | | | | | | |
| | 383 (19700) | 547 | 4.3 | 0.31 | 552 | 0.3 | 537 | 7.3 |
| | 286 (13150) | (546)[c] | | | | | | |
| | 240 (20500) | | | | | | | |

[a] For the absorption, the maxima (or shoulders) of the main bands are given. The spectra were measured in deuterated acetonitrile, unless otherwise stated. The emission data shown have been obtained by exciting the samples at the maximum of their respective lowest-energy absorption band. [b] In EtOH/MeOH 4:1 v/v. [c] In dichloromethane. [d] Upon exciting at 410 nm, an emission maxima at 478 nm is found. [e] On exciting at 410 nm, an emission maxima at 490 nm is found. [f] On exciting at 410 nm, an emission maxima at 490 nm is found a with 1.6-ns lifetime (for details, see the text).

All of the compounds exhibit a relatively intense emission spectrum (Table 2, Figure 5) in both acetonitrile or dichloromethane solutions at room temperature, with lifetimes in the nanosecond timescale (apart from **5**, whose lifetime is slightly shorter). The luminescence data were independent of the excitation wavelength used, within the range 300–400 nm for **1**–**5** and 320–520 nm for **6**. The luminescence data, which are reported in Table 2 and Figure 5, have been obtained by exciting at the maximum of the lowest energy absorption band or at higher energies. However, for **1**–**4**, when the excitation wavelength is set at the extreme red-edge of the lowest energy-absorption band, somewhat different luminescence data are obtained. The discussion in this section concerns the luminescence data obtained for all the compounds by exciting at the absorption maxima or at higher energies. The dependence of the emission spectra on excitation wavelength, in particular for **4**, taken as a representative example, will be discussed later.

For all the compounds except **6**, the emission spectrum is significantly redshifted compared with the absorption spectrum, indicating a strong Stokes shift, which suggests a large structural change in the excited state compared with the ground

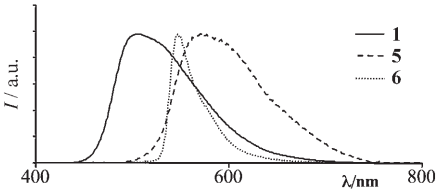


Figure 5. Emission spectra of **1**, **5**, and **6** in acetonitrile at room temperature (excitation wavelength: 360 nm, 370 nm, and 525 nm, respectively). The spectra shown are uncorrected for photomutiplier response. For corrected emission maxima, see Table 2.

  

state. Such a structural change agrees with the ultrafast excited-state intramolecular-proton-transfer process from the Franck–Condon state, which is typical of such species.[6,11,12] As for the absorption maxima (see above), the emission maxima of **3**–**5** are redshifted compared with those of **1** and **2** as a consequence of the presence of the alkynyl substituents. Such a red shift is more significant for compound **5**, which contains the terpyridine moiety. This suggests that such a moiety plays the role of a strong electron-withdrawing group, stabilizing the emitting state. This finding agrees with the solid-state planar structure of **5** (see above), which indicates facile delocalization throughout all of the molecule.

A possible question is whether a double proton transfer occurs in the excited state in **1**–**5** or if the substitution on the bipyridyl rings limits the process to a single-proton transfer process. In fact, the presence of an electron-withdrawing group at the 6-substituted position of the $BP(OH)_2$ species has been found to limit the process to a single proton transfer.[13g] For example, the emission of the single-proton-transfer product of the parent species [2,2′-bipyridyl]-3,3′-diol in cyclohexane, recorded by femtosecond fluorescence up-conversion, peaks at 568 nm,[13c] which is significantly redshifted compared with the emission of the double-proton-transfer species (510 nm). However, these data promptly suggest that for **1** and **2**, emission comes from the double transfer form (see Table 2). The same conclusion can also be drawn for **3**–**5**: in fact, as the absorption spectra suggest that in species **3**–**5**, the lowest energy transition (and the corresponding excited state(s)) involves a state with some delocalization (see above), both the emissions from mono- and di-proton-transfer tautomeric forms of **3**–**5** should be redshifted compared with the corresponding emission of the parent unsubstituted species [2,2′-bipyridyl]-3,3′-diol. As a result, the emission spectra of **3**–**5** reported in Table 2 are consistent only with a double-proton-transfer product. The question "double versus single proton transfer" cannot be discussed for **6** as the luminescence data refer to a different subunit than that of the bipyridyldiol subunit (see below).

The redshift of the emission band of **3** and **4** with respect to **1** and **2** is coupled with prolonged lifetimes and decreased quantum yields (see Table 2). This indicates that both radiative and radiationless processes are slower for **3** and **4** compared with **1** and **2**. Slowed, radiationless processes can be due to delocalization of the emitting state into the alkynyl group; such a delocalization is expected to reduce structural distortion of the excited-state geometry with respect to the ground state, thereby decreasing Franck–Condon factors for radiationless decay. The reduction of the radiative decay rate constants is less immediate to justify. The luminescence lifetime data at 77 K (see below) could help in this regard. Usually, luminescence lifetimes are longer at 77 K than at room temperature as a consequence of deactivation (or reduction) of some vibrational modes (including solvent-coupled modes) that contribute to the radiationless decay. Compounds **1**, **2**, **5**, and **6** follow this rule (Table 2), but **3** and **4** are an exception. The situation is somewhat reminescent of that reported for $Cu^I$ polypyridine complexes.[18] Tentatively, and analogously to $Cu^I$ complexes, this could be explained assuming that the excited states responsible for the emission of **3** and **4** are not exactly the same at room temperature and at 77 K. At room temperature, two closely lying excited states could contribute to the emission process, and the observed decay constants would be average values. Upon passing to 77 K, one of such two states could be preferentially stabilized so that the emission properties in this condition could not be directly compared with those at room temperature. The slight redshift of the emission spectra of **3** and **4** on passing from room temperature to 77 K (see Table 2), contrary to what usually occurs, seems to support this hypothesis. However, we currently have no clear-cut data to support this hypothesis, so it should be considered with care. Temperature-dependent luminescence experiments could probably answer this question, but these experiments have not been performed because of technical reasons.

For the terpy-containing species **5**, both luminescence lifetimes and quantum yields are reduced compared with **1** and **2** (Table 2). In this case, the energy-gap law is most likely responsible for such an effect.

Compound **6** contains another well-known luminophore, the boron-dipyrromethene dye,[2,19,20] whose emission is typical of this latter subunit. Interestingly, the excitation spectrum of **6** closely matches the corresponding absorption spectrum, indicating that complete energy transfer from the dihydroxy-bipyridine moiety to the boron-dipyrromethene luminophore takes place. This is in agreement with the fact that the lowest-energy excited state of **6** involves the diboron-pyrromethene subunit (compare emission data of **3**, **4**, and **6**, Table 2). As far as the mechanism of this energy-transfer process is concerned, the quite good overlap between donor emission and acceptor absorption, as inferred from the experimental data (see Table 2 and Figures 4 and 5), strongly suggests that a Coulombic energy-transfer process could be dominant.

For all the species, luminescence properties in dichloromethane are quite close to those in acetonitrile (see Table 2 for emission maxima), confirming, as for the case of the absorption spectra, that charge-transfer contributions are small. This point is less valid for **5**, in which the presence of the terpyridine moiety, which is a good electron-acceptor group, confers apartial charge-transfer character to the emitting state.

All the compounds also emit at 77 K in a rigid matrix in which the emission spectra are very close to the corresponding spectra at room temperature. This highlights that the excited-state intramolecular proton transfer also occurs in a rigid matrix. In these experimental conditions, the same differences as were already discussed for the room-temperature luminescence with respect to emission energy shifts among **1**–**5** are found and the same line of discussion can be made. Similarly, emission of **6** is different from the others and can be assigned to a different excited state, the lowest-energy singlet level of the boron-dipyrromethene subunit.

  

Solid-state luminescence has also been performed (see Table 2). For all of the species, the results are again similar to those obtained in solution, with the noticeable difference that the luminescence spectra are redshifted in the solid state. In addition to indicating that the excited-state intramolecular proton transfer of the studied compound takes place even in the solid state without requiring solvent assistance, this result also suggests that the relaxed excited state (that is the excited-state product of the intramolecular proton transfer) is more stable in the solid state that in the solution. This is most likely because of crystal-packing effects. The redshift is less effective for **6** as expected as the luminophore of this species is different in origin (that is, it is the bodipy dye).

**Luminescence spectra as a function of excitation wavelength**: As mentioned above, the luminescence spectra of **1**–**4** are excitation-wavelength dependent: for example, although excitation in the maximum of the lowest-energy absorption band leads to emission spectra that can be attributed to the relaxed states produced by the ESIPT process (see Table 2) by exciting **4** at 410 nm (i.e., at the red edge of the lowest-energy absorption band), an additional emission with a maximum at 490 nm is obtained with a lifetime of 1.6 ns (see Figure 6). By making measurements of four solutions of **4** that are isoabsorbitive at four different wavelengths, it is clear (Figure 6) that an increase in the high-energy emission corresponds to a decrease in the low-energy emission, suggesting that emission at 490 nm occurs with loss of the emission at 535 nm, that is, the two excited states are correlated and population of one state leads to depopulation of the other. The obvious parent of the low-energy emission (e.g., of the emission originating from the excited state produced by the ESIPT process) is the Franck–Condon excited state (the $S_1$ state), which precedes the proton-transfer process. Such a state could be fluorescent, although, it is normally deactivated by ESIPT. However, as recently reported,[14] the ESIPT process can be coupled to skeletal motions in some related species like 2-(2′-hydroxyphenyl)benzothiazole.[14b–d] Assuming that the ESIPT process can also be coupled to skeletal motions in the present systems, substitution of the 4-position of the bipyridyl rings could affect the skeletal motions so that ESIPT can only occur (or prevalently occurs) when enough vibrational energy is injected into the Franck–Condon state by light excitation, making the ESIPT process excitation-wavelength dependent. Substitution at the 4-position affects the excited-state properties of the bi-

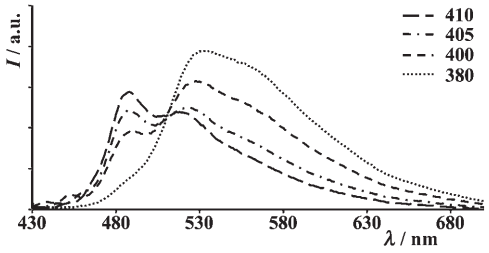


Figure 6. Luminescence spectra of **4** in acetonitrile at different excitation wavelengths (380, 400, 405, 410 nm). The spectra refer to four different solutions that are isoabsorbitive at the given wavelengths.

pyridyldiol subunit as can be seen by the red shift in the absorption and luminescence properties for the species containing the electron-withdrawing alkynyl substituents (compare data of **3** and **4** with those of **1** in Table 2). This line of reasoning leads to assignment of the emission at 490 nm of **4** (and the analogous emission of **1**–**3** in which qualitatively similar results are found) to an excited state that precedes the complete ESIPT process, most likely the Franck–Condon state. Within this hypothesis, the situation can be pictured as is shown in Figure 7 a. The excitation spectra of **4**, recorded at different emission wavelengths, agree with this hypothesis (Figure 8): when the excitation spectrum is recorded at 560 nm, it yields a spectrum that is quite similar to the absorption spectrum, but missing a contribution at the red-edge limit. This is in agreement with activation of the ESIPT process by vibrationally rich excited states; when it is recorded at 480 nm, it yields a prominent contribution in the region 400–450 nm, which corresponds to the red-edge absorption of **4**.[21] However, the experimental findings would also be fitted by considering the presence of an additional excited state that could be directly populated (preferentially or exclusively) by light excitation mostly between 400 and 450 nm, although with small molar absorption coef-

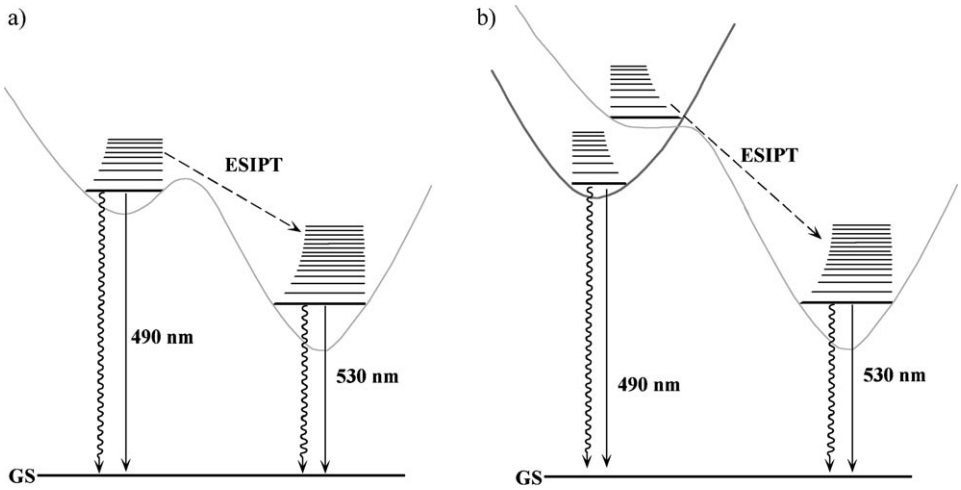


Figure 7. Proposed schematic representations of the excited-state decay processes in **4**. a) Hypothesis based on vibrational dependence of the ESIPT process. b) In this case, there is an additional excited state that decays independently from the state undergoing ESIPT. GS = ground state.

  

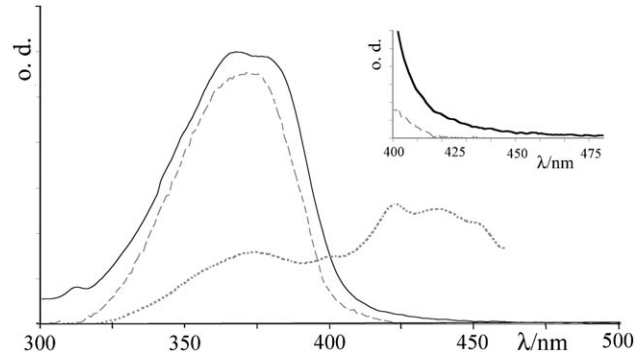


Figure 8. Excitation spectra of **4** recorded at 480 nm (——) and at 560 nm (-----) compared with the absorption spectrum (–•–•). Solvent: acetonitrile. O.d. = optical density.

ficients. Such a state would decay directly to the ground state without undergoing the ESIPT process. The excitation wavelength dependence of the luminescence behavior of **1**–**4** would therefore be due to competitive absorption by two different electronic states that undergo different and independent decay routes. This situation is shown in Figure 7b. To decide in favor of one of these two cases would probably require detailed temperature-dependent studies or a theoretical approach, both of which are not within the scope of this paper.

The luminescence properties of **5** and **6** do not show any excitation wavelength dependence: this is somewhat obvious for **6** as the emission comes from a lower-lying excited state to that which the bipyridyldiol unit deactivates. In compound **5**, the attached terpyridyl unit causes a large perturbation on the nature of the excited state (see absorption and emission spectra of **5**, which are strongly redshifted even compared with those of **1**–**4**, Table 2), so it is not surprising that the excited state behavior of this species does not show excitation wavelength dependence that is different from the closely related **1**–**4** species.

**Luminescence in the presence of zinc salts**: Luminescent compounds whose excited-state properties undergo noticeable changes in the presence of suitable species are extensively investigated for sensing purposes.[1e] To exploit the potential of the title compounds in this regard, we studied the photophysical properties of some representative compounds of this series, namely **4** and **5**, in the presence of zinc(II) ions in acetonitrile. For these experiments, zinc triflate was employed.

The presence of $Zn^{II}$ ions has slight effects on the absorption spectrum of **4** in acetonitrile (Figure 9): in particular, the absorption band maximizing at 370 nm decreases and a new absorption grows up in the 400–480 nm range until a Zn/**4** molecular ratio that slightly exceeds 1:1 is reached. A further increase of zinc triflate leads to a reverse effect until the 2:1 Zn/**4** molecular ratio is reached, and then further zinc addition does not have any sizeable effect. Plotting the absorption changes as a function of the Zn/**4** molecular ratio

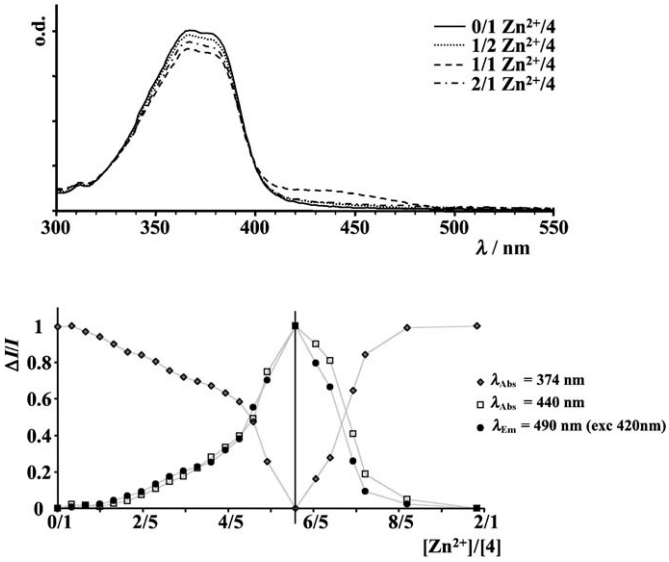


Figure 9. Top: absorption changes of **4** in acetonitrile upon zinc triflate addition. Bottom: titration curves for the absorption and emission changes. $[\mathbf{4}] = 1.0 \times 10^{-5}$ M. The gray vertical line is a guide to identify the first step of the process. $\Delta I/I$ indicates absorption or emission values.

(Figure 9, bottom) indicates that changes at 370 nm and at 420 nm refer to the same processes (i.e., a change in the 370 nm absorbance corresponds to a spectroscopic change in the 420 nm absorbance). The existence of two consecutive processes indicates that two zinc cations consecutively interact with **4**. Any attempts to calculate association constants for the formation of adducts by using Specfit (spectrum Software Associates, Chapel Hill, NC, 1996) were unsuccessful, so our interpretation of the results has to be considered as tentative.

The emission spectra are also affected by the presence of zinc triflate, both excited at 380 nm (which allows for an effective ESIPT process in **4** and therefore yields emission at 530 nm, see above) and at 420 nm (where emission at 490 nm dominates). Upon excitationing at 380 nm (Figure 10, top) the presence of zinc(II) ions leads to the appearance of an emission peak at 490 nm, which increases until the 1:1 **4**/Zn molecular ratio is reached. Further zinc triflate addition leads to a decrease in the emission until a 1:2 molecular ratio of **4**/Zn is obtained. Even upon further zinc addition, the emission spectrum remains constant. Notably, the emission at about 530 nm remains roughly constant during the titration process: this suggests that the presence of a $Zn^{II}$ cation improves the emitting properties of the state that is responsible for the 490 nm emission without affecting the 530 nm emission; therefore the ESIPT process is not inhibited by the presence of zinc salts. Note that this result is consistent with both hypotheses in Figure 7. The decrease in the 490 nm emission intensity upon addition of the second zinc(II) ion can be rationalized simply by assuming that the 490 nm emission state in the **4** adduct that contains two zinc ions has worse emitting properties than in the **4** adduct containing one zinc(II) ion.

  

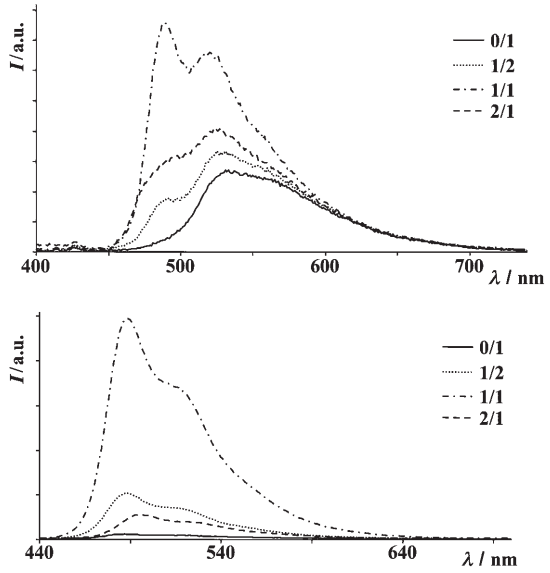


Figure 10. Luminescence spectra of **4** in acetonitrile in the presence of zinc triflate. The excitation wavelength is 380 nm (top) and 420 nm (bottom). $[\mathbf{4}] = 1.0 \times 10^{-5}$ M.

Upon exciting **4** at 420 nm **(**Figure 10, bottom), the addition of zinc triflate leads to an increase in the original emission at 490 nm until it reaches the 1:1 molecular ratio; the emission peak decreases when zinc(II) is increased to the 1:2 **4**/Zn ratio, which is in agreement with consecutive formation of 1:1 and 1:2 **4**/$Zn^{II}$ adducts and the results obtained by exiting at 380 nm. Luminescence titration curves (see Figure 9, bottom) are in line with the absorption titration curves.

Before investigating compound **5** in which two subunits are potentially capable of interacting with cations, we performed a similar experiment on 4′-ethynyl-2,2′:6′,2″-terpyridine (**T**), which is used as a model for the properties of the terpyridine-type chelating subunit of **5**. The absorption spectrum of **T** is strongly modified by the presence of $Zn^{II}$ (Figure 11, top): in particular, the low-energy absorption is significantly redshifted and increased, which is a common consequence of $Zn^{II}$ chelation by terpyridine subunits.[22] Luminescence is also strongly changed (Figure 11, center): it is redshifted and increased according to the stabilization of the terpyridine-based π–π* state. Furthermore, deactivation of some modes promotes radiationless transition in free **T**. Noteably, both absorption and luminescence changes require one equivalent of zinc triflate to arrive at the end of the process, indicating formation of a 1:1 **T**/Zn adduct (see Figure 11, bottom).

For compound **5**, the addition of $Zn^{II}$ until it reaches a 1:1 **5**/Zn molecular ratio has strong effect on both the absorption spectrum (Figure 12, top) and the luminescence spectrum (Figure 12, center); in particular, the emission at 570 nm is totally quenched. Further addition of zinc salts does not modify the absorption and emission spectra anymore (Figure 12, top), which suggests the formation of a 1:1

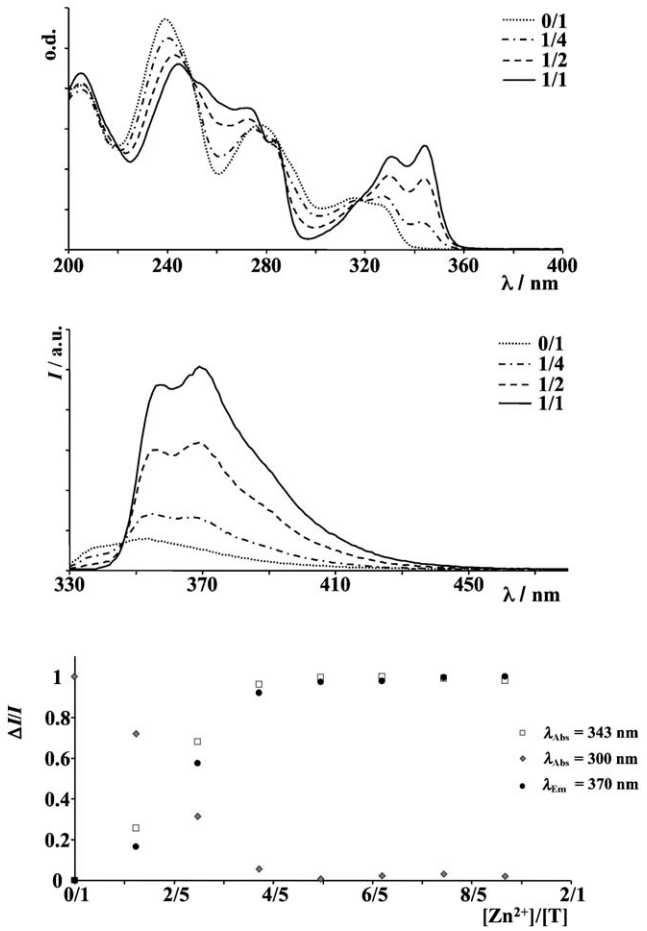


Figure 11. Absorption (top) and emission (center) changes of **T** in acetonitrile upon the addition of zinc triflate. Bottom: titration curves for the absorption and emission changes. $[\mathbf{T}] = 3.2 \times 10^{-5}$ M.

**5**/Zn adduct. As **5** contains several sites that are in principle available for zinc(II) coordination, one could ask which site is effective. It was impossible to determine reliable association constants for the various adducts of $Zn^{II}$ with **4**, **5**, and **T**. However, comparison between the absorption titration curves relative to the formation of the 1:1 **T**/Zn, **4**/Zn, and **5**/Zn adducts (Figure 13) can be instructive in this regard: it is clear that the titration curve of the formation of the 1:1 **5**/Zn species is quite close to that of formation of the 1:1 **T**/Zn, suggesting that in the **5**/Zn adduct, the zinc(II) ion is coordinated to the terpyridine site. This hypothesis also agrees with the large effects on the absorption spectrum of **5** upon zinc addition. These effects are similar to that of the **T**/Zn adduct and different to what happens with the **4**/Zn adduct. The quenching of the emission in the **5**/Zn adduct, which disagrees with the emission-intensity enhancement found for both **T**/Zn and **4**/Zn adducts, can be due to the presence of a new (low-energy and nonemissive) charge-transfer state that could be stabilized in the **5**/Zn adduct. In this case, the donor orbital would be centered on the bipyridyldiol subunit and the acceptor orbital on the $Zn^{II}$-complexed terpyridine unit.

  

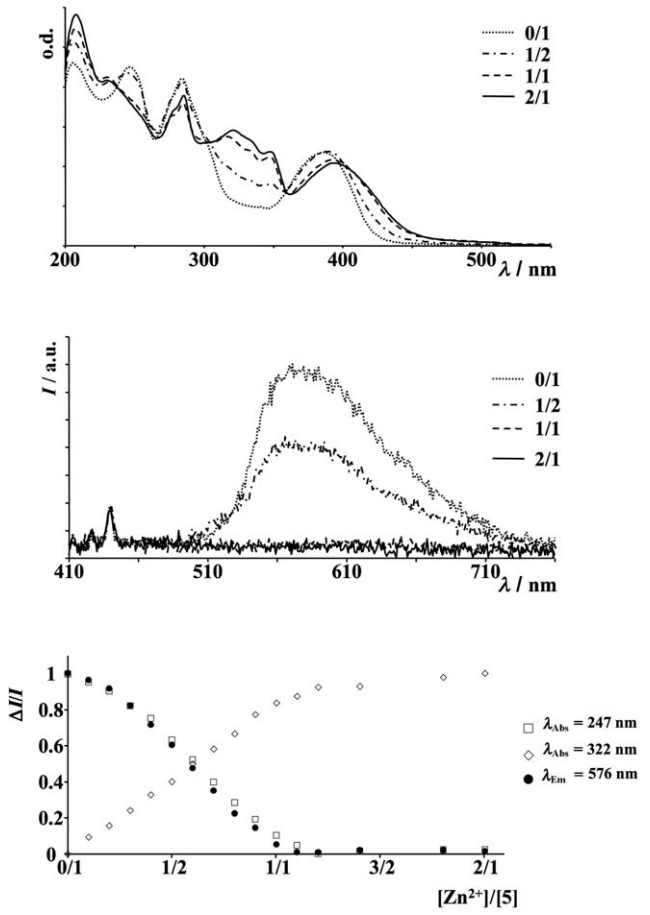


Figure 12. Absorption (top) and emission (center) changes of **5** in acetonitrile upon zinc triflate addition. Bottom: titration curves for the absorption and emission changes. $[\mathbf{5}] = 7.8 \times 10^{-6}$ M.

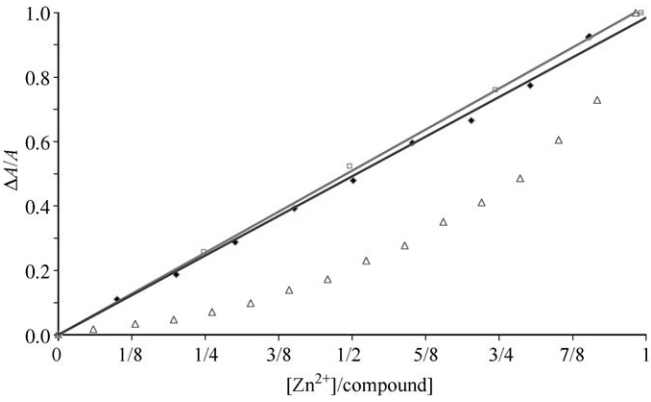


Figure 13. Titration curves for the absorption changes upon zinc triflate addition for **4** (△, $\lambda_{Abs} = 370$ nm), **T** (□ (——), $\lambda_{Abs} = 343$ nm), and **5** (◆ (-----), $\lambda_{Abs} = 345$ nm). The lines act as a visual guide.

Complexation of $Zn^{II}$ by the terpyridine unit of **5** still leaves the bipyridyldiol site(s) uncomplexed, however, no further $Zn^{II}$ interaction seems to occur: it is most likely that upon terpy-centered $Zn^{II}$ complexation, the coordination ability of the bipyridyldiol subunit is decreased so that $Zn^{II}$ coordination by the bipyridyldiol becomes inefficient.

## Conclusion

We have succeed in the chemical monofunctionalization at the 4-position of the [2,2′-bipyridine]-3,3′-diol ($BP(OH)_2$) platform without the need for protection steps. The extension of the delocalization that is promoted by the ethyne connection induces a bathochromic shift and allow the introduction of useful modules, such as energy acceptor or chelating groups. All of the species are emitting, both at room temperature in fluid solution and in the solid state and at 77 K in rigid matrix, from an excited state that is produced following ESIPT. In some cases, excitation-wavelength luminescence is found and is attributed to 1) inefficiency of the ESIPT process in selected compounds in which not enough vibrational energy is introduced in the Franck–Condon state populated by light excitation or 2) the presence of an additional excited state, which mainly absorbs within the 400–450 nm range and decays directly to the ground state. For some species, the effect of the addition of zinc salts was investigated and it has been shown that the addition of zinc salts induces significant fluorescence changes. These changes are a consequence of the consecutive formation of a 1:1 and a 1:2 molecular ratio of ligand/zinc adducts that are formed by the coordination of $Zn^{II}$ ions by the bipyridyldiol moieties. The exception is the presence of an additional terpyridine subunit, which coordinates the $Zn^{II}$ ion preferentially in a 1:1 molecular ratio and thereby inhibits further $Zn^{II}$ interaction with the bipyridyldiol site. In the mixed bodipy/$BP(OH)_2$ fluorophore (compound **6**), fast and quantitative energy transfer occurs, resulting in the unique bodipy emission. Additional chemical modifications at the 6,6′-, 5,5′-, and 4,4′-positions of the $BP(OH)_2$ core is now envisaged to tune the coordination abilities and luminescence properties of these ligands. The use of this family of dyes as photoactive components in sophisticated multichromophoric architectures is currently in progress.

## Experimental Section

**General methods and equipment**: All chemicals were used as received from commercial sources without further purification unless otherwise stated. $NEt_3$ was allowed to stand on KOH pellets prior to use. $^1$H NMR (200.1 or 300.1 MHz) and $^{13}$C NMR (75.5 MHz) spectra were recorded at room temperature on a Bruker AC200 or Advance 300 MHz spectrometer by using perdeuteriated solvants as the internal standards. FTIR spectra were recorded as KBr pellets. UV/Vis absorption spectra were recorded on a Perkin-Elmer Lamda Uvikon 933 spectrophotometer or with a Jasco 560 spectrophotometer. Fast atom bombardement (FAB, positive mode) mass spectra were recorded with ZAB-HF-VB analytical apparatus with *m*-nitrobenzyl alcohol (*m*-NBA) as the matrix. Chromatographic purifications were performed by using 40–63 μm silica gel. TLC was performed on silica gel plates coated with fluorescent indicator. For the calculation of the association constants, the software used was Specfit (spectrum Software Associates, Chapel Hill, NC, 1996). Steady-state luminescence spectra were recorded with a Horiba Jobin-Yvon Fluoromax P spectrofluorimeter equipped with a Hamamatsu R3896 photomultiplier and were corrected for photomultiplier response by using a program purchased with the fluorimeter. Emission lifetimes were measured with an Edinburgh OB-900 single-photon-counting spectrometer equipped with a

  

Hamamatsu PLP-2 laser diode (pulse width at 408 nm, 59 ps) and with a PicoQuant PDL 800-D pulsed laser diode (pulse width at 308 nm, 50 ps). The emission decay traces (emission lifetimes measured at approximately the emission maximum wavelengths) were analyzed by Marquadt algorithm. For each measurement, at least five determinations were carried out. The values reported are averaged lifetimes of these determinations. Each single determination value does not differ from the averaged values by more than 10%. Luminescence quantum yields have been calculated by using the optically dilute method;[23a] as the reference, $[Ru(bpy)_3]^{2+}$ (bpy = 2,2′-bipyridine) in aerated water was used ($\Phi = 0.028$[23b]). Each one of the reported values is averaged over three independent quantum-yield measurements by using different excitation wavelengths. Each measurement differs from the averaged value by less than 15%. Emission spectra and lifetimes for **5** and **6** are independent of excitation wavelength within the experimental ranges used (300–420 nm for **5**, 300–520 nm for **6**). The luminescence spectra in the presence of different concentrations of zinc salts have been recorded by exciting the samples at the corresponding isosbestic points. The solid-state samples for luminescence experiments have been prepared by evaporating an acetonitrile solution of the corresponding compound on a quartz platform, which was then located in the fluorimeter cuvette holder.

Experimental uncertainty for absorption-spectra maxima is 2 nm, for molar absorption is 10%, for luminescence emission maxima is 4 nm, for lifetime is 10%, and for quantum yields is 20%.

Crystal data for compound **5**: $[2(C_{29}H_{21}N_5O_2), CH_2Cl_2]$; $M_r = 1027.94$, monoclinic, space group $P21$, $a = 7.774(2)$, $b = 32.603(4)$, $c = 10.219(2)$ Å, $b = 105.362(4)°$, $V = 2497.5(9)$ Å$^3$, $Z = 2$, $Z' = 2$, $\rho_{calcd} = 1.367$ g cm$^3$, ($Mo_K = 0.191$ mm; $F(000) = 1068$), $T = 293$ K.

The X-ray diffraction data were recorded from an elongated orange plate of dimensions $0.36 \times 0.18 \times 0.12$ mm$^3$ at ambient temperature on an Enraf Nonius Kapp.[24] Absorption correction on structure factors was performed following the multiscan method as implemented with SCALEPACK.[25] The structure was solved by direct methods by using SIR97[26] software and all non-hydrogen atoms were refined with anisotropic displacement parameters by using SHELX-L97d by full-matrix least squares on $F^2$ values. Hydrogen atoms were located from Fourier difference syntheses and then treated as riding atoms, with $U_{iso}$ set to 1.2 times that of the attached C atom (1.5 when methyl group was present). Convergence for 677 variable parameters by least-squares refinement on $F^2$ with $w = 1/[(2(F_o^2) + (0.0806P)2 + 1.1875P]$, where $P = (F_o^2 + 2F_c^2)/3$ for 3620 reflections with $I > 2\sigma(I)$ was reached at $R = 0.0585$ and $wR = 0.1398$ with a goodness-of-fit of 1.043. The final difference Fourier map has maximum positive and negative peaks (associated with the dichloromethane molecule) of 0.281 and −0.240 e, respectively.

CCDC-619425 contains the supplementary crystallographic data for this paper. These data can be obtained free of charge from The Cambridge Crystallographic Data Centre via www.ccdc.cam.ac.uk/data_request/cif.

**Reagents**: All reagents were used directly as obtained commercially unless otherwise noted. NBS, trimethylsilyl acetylene, and KF were purchased from Aldrich Chemical Co., Inc.

**Materials**: 3,3′-Dihydroxy-6,6′-dimethyl-2,2′-bipyridine,[27] $[Pd(PPh_3)_4]$,[28] 4′-trifluorosulfonato-2,2′:6′,2″-terpyridine,[29] and 4,4-difluororo-8-(*p*-iodophenyl)-1,3,5,7-tetramethyl-2,6-diethyl-4-bora-3*a*,4*a*-diaza-s-indacene[16] were synthesized according to previously reported literature procedures.

**4-Bromo-3,3′-dihydroxy-6,6′-dimethyl-2,2′-bipyridine (2)**: NBS (0.82 g, 4.6 mmol) was added portionwise to a solution of **1** (1 g, 1.6 mmol) in a $CH_2Cl_2$/DMF (1:2, 30 mL) mixture at 0°C. The slurry was stirred at 0°C over 1 h, then left to warm to room temperature over 2 h. Water (50 mL) was then added and the mixture extracted with dichloromethane. The organic layer was washed with water, dried over $MgSO_4$, and then the solvent was removed. Purification with chromatography ($SiO_2$, $CH_2Cl_2$) afforded the desired compound as shiny yellow powder (1.01 g, 75%).

$^1$H NMR (200 MHz, $CDCl_3$): ($\delta = 16.23$ (s, 1H), 14.30 (s, 1H), 7.40 (s, 1H), 7.26 ($AB_{sys}$, 2H, $J_{AB} = 2.9$ Hz , $\nu_0\delta = 33.3$ Hz), 2.52 (s, 3H), 2.51 ppm (s, 3H); $^{13}$C{$^1$H} NMR (75 MHz, $CDCl_3$): 155.9, 151.6, 144.7, 144.5, 138.4, 137.4, 127.7, 126.8, 125.2, 122.3, 22.5, 22.4 ppm; IR(KBr): $\tilde{\nu} = 3071$, 2923, 2488 (br), 1930, 1766, 1603, 1571, 1486, 1380, 1294, 1229, 1131 cm$^{-1}$; UV/Vis ($CH_3CN$) $\lambda_{max}$ ($\varepsilon$): 356 (17900), 250 nm; HRMS-FAB$^+$ *m*/*z* (nature of peak, relative intensity): 297.1 ($[M+H]^+$, 99), 295.1 ($[M+H]^+$, 278.1 ($[M-OH]^+$, 20); elemental analysis calcd (%) for $C_{12}H_{11}BrN_2O_2$: C 48.84, H 3.76, N 9.49; found: C 48.68, H 3.56, N 9.21.

**4-Trimethylsilyethynyl-3,3′-dihydroxy-6,6′-dimethyl-2,2′-bipyridine (3)**: A solution of **2** (0.18 g, 0.6 mmol) in a triethylamine/THF (1:1, 6 mL) mixture was thoroughly degassed with argon for 30 min. $[Pd(PPh_3)_4]$ and trimethylsilylacetylene were then added, and the slurry was stirred at 60°C, under Ar, for one day. Water was then added (10 mL) and the mixture extracted with dichloromethane. The organic layer was dried over $MgSO_4$ and then the solvent was removed. Purification with chromatography ($SiO_2$, $CH_2Cl_2$/cyclohexane, 8:2 to 10:0) gave the titled compound as a yellow solid (0.16 g, 52%).

$^1$H NMR (200 MHz, $CDCl_3$): ($\delta = 15.77$ (s, 1H), 14.44 (s, 1H), 7.20 ($AB_{sys}$, 2H, $J_{AB} = 8.5$ Hz , $\nu_0\delta = 38.1$ Hz), 7.18 (s, 1H), 2.49 (s, 3H), 2.46 (s, 3H), 0.29 ppm (s, 9H); $^{13}$C{$^1$H} NMR (75 MHz, $CDCl_3$): 154.8, 154.1, 144.7, 143.8, 138.7, 137.1, 127.0, 126.6, 125.0, 121.0, 103.9, 98.6, 22.5, 22.4, −0.1 ppm; IR(KBr): $\tilde{\nu} = 2960$, 2923, 2503, 2153, 1729, 1591, 1482, 1383, 1298, 1235 cm$^{-1}$; UV/Vis ($CH_3CN$) $\lambda_{max}$, nm ($\varepsilon$) = 378 (22400), 238 (28000); HRMS-FAB$^+$ *m*/*z* (nature of peak, relative intensity): 313.1 ($[M+H]^+$, 100), 239.2 ($[M-TMS]^+$, 25); elemental analysis calcd (%) for $C_{17}H_{20}N_2O_2Si$: C 65.35, H 6.45, N 8.97; found: C 65.15, H 6.18, N 8.59.

**4-Ethynyl-3,3′-dihydroxy-6,6′-dimethyl-2,2′-bipyridine (4)**: KF (0.3 g, 5 mmol) in methanol (5 mL) was added to a solution of **3** (0.16 g, 0.5 mmol) in $CH_2Cl_2$ (5 mL). The mixture was stirred at RT until complete deprotection was observed by TLC. Purification with chromatography ($SiO_2$, $CH_2Cl_2$) gave the pure desired compound (0.7 g, 57%).

$^1$H NMR (200 MHz, $CDCl_3$): ($\delta = 15.96$ (s, 1H), 14.32 (s, 1H), 7.22 ($AB_{sys}$, 2H, $J_{AB} = 8.2$ Hz , $\nu_0\delta = 38.5$ Hz), 7.20 (s, 1H), 3.55 (s, 1H), 2.50 (s, 3H), 2.46 ppm (s, 3H); $^{13}$C{$^1$H} NMR (75 MHz, $CDCl_3$): 155.3, 153.5, 144.7, 144.0, 138.8, 138.0, 127.0, 126.8, 125.1, 121.9, 85.6, 22.7, 22.6 ppm; IR(KBr): $\tilde{\nu} = 3306$, 2957, 2924, 2855, 2503 (br), 2110, 1931, 1728, 1479, 1297, 1234 cm$^{-1}$; UV/Vis ($CH_3CN$) $\lambda_{max}$, nm ($\varepsilon$) = 370 (20200), 274 (95000); HRMS-FAB$^+$ *m*/*z* (nature of peak, relative intensity): 240.1 ($[M+H]^+$, 100); elemental analysis calcd (%) for $C_{14}H_{12}N_2O_2$: C 69.99, H 5.03, N 11.66; found: C 69.70, H 4.71, N 11.30.

**4-(2,2′:6′,2″-Terpyridine-4′-ethynyl)-3,3′-dihydroxy-6,6′-dimethyl-2,2′-bipyridine (5)**: A solution of **5** (0.04 g, 0.17 mmol) and 4′-trifluorosulfonato-2,2′:6′,2″-terpyridine (0.075 g, 0.2 mmol) in a THF/triethylamine (1:1, 5 mL) mixture was thoroughly degassed with argon for 20 min. $[Pd(PPh_3)_4]$ (8 mg, 6% mol) was then added and the mixture heated at 60°C under argon, overnight. Purification with chromatography ($SiO_2$, $CH_2Cl_2$) gave the pure desired compound (0.05 g, 62%).

$^1$H NMR (300 MHz, $CDCl_3$): ($\delta = 15.84$ (s, 1H), 14.43 (s, 1H), 8.73–8.71 (m, 2H), 8.67 (s, 2H), 8.62 (d, 2H, $^3J = 7.9$ Hz), 7.87 (td, 2H, $^3J = 7.7$ Hz, $^4J = 1.8$ Hz), 7.37–7.33 (m, 2H), 7.29 (s, 1H), 7.24 ($AB_{sys}$, 2H, $J_{AB} = 8.3$ Hz , $\nu_0\delta = 59.5$ Hz), 2.55 (s, 3H), 2.54 ppm (s, 3H); $^{13}$C{$^1$H} NMR (75 MHz + DEPT, $CDCl_3$): 155.7, 155.6, 154.9, 154.1, 149.2 (CH), 144.7, 143.9, 138.9, 138.1, 136.8 (CH), 132.6, 126.7 (CH), 126.5 (CH), 125.0 (CH), 124.0 (CH), 123.1 (CH), 121.2 (CH), 120.3, 95.3 (C≡C), 87.5 (C≡C), 22.7 ($CH_3$), 22.6 ($CH_3$) ppm ; IR(KBr): $\tilde{\nu} = 3054$, 2922, 2538 (br), 1792, 1582, 1563, 1466, 1387, 1296, 1228 cm$^{-1}$; UV/Vis ($CH_3CN$) $\lambda_{max}$, nm ($\varepsilon$) = 387 (15500), 284 (31900), 247 (29000); HRMS-FAB$^+$ *m*/*z* (nature of peak, relative intensity): 472.1 ($[M+H]^+$, 50), 239.1 ($[M-tpy]^+$, 35); elemental analysis calcd (%) for $C_{29}H_{21}N_5O_2$: C 73.87, H 4.49, N 14.85; found: C 73.42, H 3.99, N 14.49.

**4-(Ethynylphenyl-4′-[4″,4″-difluororo-8″-(1″,3″,5″,7″-tetramethyl-2″,6″-diethyl-4″-bora-3″*a*,4″*a*-diaza-s-indacene)-3,3′-dihydroxy-6,6′-dimethyl-2,2′-bipyridine (6)**: A solution of **5** (0.035 g, 0.145 mmol) and 4-iodophenyl-(4,4-difluororo-8-(1,3,5,7-tetramethyl-2,6-diethyl-4-bora-3*a*,4*a*-diaza-s-indacene) (0.08 g, 0.16 mmol) in a THF/triethylamine (1:1, 5 mL) mixture was thoroughly degassed for 20 min. $[Pd(PPh_3)_4]$ (5 mg, 6% mol) was then added and the mixture was heated oven night at 60°C under argon. Purification with chromatography ($SiO_2$, $CH_2Cl_2$) gave the pure desired compound (0.045 g, 50%).

$^1$H NMR (300 MHz, $CDCl_3$): ($\delta = 15.96$ (s, 1H), 14.43 (s, 1H), 7.74 (d, 2H, $^3J = 8.5$ Hz), 7.36–7.29 (m, 4H), 7.14 (d, 1H, $^3J = 8.5$ Hz), 2.53 (br s,

  

12H), 2.31 (q, 4H, $^3J=7.5$ Hz), 1.33 (s, 6H), 0.98 ppm (t, 6H, $^3J=7.5$ Hz); $^{13}C\{^1H\}$ NMR (75 MHz + DEPT, $CDCl_3$): 154.7, 154.2, 154.0, 144.6, 144.0, 139.1, 138.7, 138.2, 138.1, 136.6, 133.0, 132.6 (CH), 130.8, 130.5, 129.2, 128.8, 128.6 (CH), 126.7 (CH), 126.3 (CH), 125.0 (CH), 123.2, 120.8, 97.0 (C≡C), 84.5 (C≡C), 22.7 ($CH_3$), 22.6 ($CH_3$), 17.0 ($CH_2$), 14.6 ($CH_3$), 12.5 ($CH_3$), 11.9 ppm ($CH_3$); IR(KBr): $\tilde{\nu}=3052$, 2921, 2217, 1583, 1564, 1466, 1296, 1238, 1228, 1030, 1004 $cm^{-1}$; UV/Vis ($CH_3CN$) $\lambda_{max}$ ($\varepsilon$) = 525 (42200), 383 (19700), 286 (13200), 240 nm (20500); HRMS-FAB$^+$ *m/z* (nature of peak, relative intensity): 619.2 ($[M+H]^+$, 100); elemental analysis calcd (%) for $C_{37}H_{37}BF_2N_4O_2$: C 71.85, H 6.03, N 9.06; found: C 71.57, H 7.74, N 8.69.

## Acknowledgement

The University of Messina, MIUR (PRIN project no. 2006030320), Université Louis Pasteur (Strasbourg), CNRS and ANR JCJC05–42228 (GU) are acknowledged for financial support. We also thank Ugo Mazzucato and Gianna Favaro for useful discussions.

[1] The literature on this topic is too vast to be exhaustively quoted. For some examples, see: a) *Organic Electroluminescent Materials and Devices* (Eds: S. Miyata, H. S. Nalwa), Gordon and Breach, Langhorne, PA, **1996**; b) B. Valeur, *Molecular Fluorescence: Principles and Applications*, Wiley-VCH, Weinheim, **2002**; c) *Fluorescence Spectroscopy in Biology: Advanced Methods and their Applications to Membranes, Proteins, DNA and Cells* (Eds: H. Martin, H. Rudlof, F. Vlatimil), Springer, Heidelberg, **2005**; d) *Topics in Fluorescence Spectroscopy*, **1994**, *4*, special issue entitled *Probe Design and Chemical Sensing* (Ed: J. R. Lakowicz); e) *J. Mater. Chem*, **2005**, *15*, special issue entitled: *Fluorescent Sensors* (Eds: A. P. De Silva, P. Tecilla); f) *Handbook of Photochemistry, Third Edition* (Eds: M. Montalti, A. Credi, L. Prodi, M. T. Gandolfi), CRC Press, New York, **2006**.

[2] R. P. Haughland, The *Handbook: a guide to Fluorescent Probes and Labelling Technologies*, 10th ed, Molecular Probes, Eugene, OR, **2005**.

[3] D. Gormi, J. Heldt, M. Kasha *J. Phys. Chem.* **1990**, *94*, 1185.

[4] D. LeGourriérec, V. Kharlanov, R. G. Brown, W. Rettig, *J. Photochem. Photobiol. A: Chemistry* **1998**, *117*, 209.

[5] W. E. Brewe, M. L. Martinez, P.-T. Chou *J. Phys. Chem.* **1990**, *94*, 1915.

[6] H. Langhals, S. Pust, *Chem. Ber.* **1986**, *118*, 4674.

[7] a) L. Kaczmarek, P. Borowicz, A. Grabowska, *J. Photochem. Photobiol. A: Chem.* **2001**, *138*, 159; b) L. Kaczmarek, B. Zagrodzki, B. Kamienski, M. Pietrzak, W. Schilf, A. Les *J. Mol. Struct.* **2000**, *553*, 61.

[8] C. Goze, G. Ulrich, L. Charbonnière, R. Ziessel *Chem. Eur. J.* **2003**, *9*, 3748.

[9] R. Ziessel, C. Goze, G. Ulrich, M. Césario, P. Retailleau, A. Harriman, J. P. Roston, *Chem. Eur. J.* **2005**, 11, 7366.

[10] For examples of fundamental and potentially applicative papers on $BP(OH)_2$-type molecules, see: a) A. Weller, *Z. Electrochem.* **1956**, *60*, 1144; b) S. J. Formosinho, L. G. Arnaut, *J. Photochem. Photobiol., A: Chem.*, **1993**, *75*, 21; c) N. Agmon, *J. Phys. Chem. A*, **2005**, *109*, 13; d) N. Basaric, P. Wan, *Photochem. Photobiol. Sci.*, **2006**, *5*, 656. For examples of fundamental and potentially applicative papers on analogous species, see: e) D. A. Parthenopoulos, D. McMorrow, M. Kasha, *J. Phys. Chem.*, **1991**, *95*, 2668; f) M. Kasha, *Acta Phys. Pol. A*, **1987**, *A71*, 717; g) F. Vollmer, W. Rettig, *J. Photochem. Photobiol. A: Chem.*, **1996**, *95*, 143; h) S. Park, O.-H. Kwon, S. Kim, S. Park, M.-G. Choi, M. Cha, S. Y. Park, D.-J. Yang, *J. Am. Chem. Soc.*, **2005**, *127*, 10070; i) M. Suresh, D. A. Jose, A. Das *Org. Lett.* **2007**, *9*, 441; j) F. Rodriguez Prieto, M. C. Rios Rodriguez, M. Mosquera Gonzales, M. A. Rios Fernandez, *J. Phys. Chem.* **1994**, *98*, 8666; k) J. C. Penedo, M. C. Rios Rodriguez, I. Garcia Lema, J. L. Perez Lustres, M. Musquera, F. Rodriguez-Prieto, *J. Phys. Chem. A* **2005**, *109,* 10189; l) S. Vazquez, M. Rodriguez, M. Musquera, F. Rodriguez-Prieto, *J. Phys. Chem. A* **2007**, *111,* 1814.

[11] A. Mordzinski, K. Kownacki, A. Les, N. A. Oyler, L. Adamowicz, F. W. Langkilde, R. Wilbrandt *J. Phys. Chem.* **1994**, *98*, 5212.

[12] a) A. U. Khan, M. Kasha *Proc. Natl. Acad. Sci. USA*, **1983**, *80*, 1767; b) J. Sepiol, H. Bulska, A. Grabowska *Chem. Phys. Lett.* **1987**, *140*, 607.

[13] a) D. Marks, H. Zhang, M. Glasbeek *J. Lumin.* **1998**, *76–77*, 52; b) A. L. Sobolewski, L. Adamowicz *Chem. Phys. Lett.* **1996**, *252*, 33; c) H. Zhang, P. van der Meulen, M. Glasbeek *Chem. Phys. Lett.* **1996**, *253*, 97; d) D. Marks, H. Zhang, M. Glasbeek, P. Borowicz, A. Grabowska *Chem. Phys. Lett.* **1996**, *275*, 370; e) D. Marks, H. Zhang, M. Glasbeek, P. Borowicz, A. Grabowska *Chem. Phys. Lett.* **1997**, *275*, 370; f) D. Marks, P. Prosposito, H. Zhang, M. Glasbeek *Chem. Phys. Lett.* **1998**, *289*, 535; g) D. Marks, H. Zhang, P. Borowicz, A. Grabowska, M. Glasbeek *Chem. Phys. Lett.* **1999**, *309*, 19.

[14] a) F. V. R. Neuwahl, P. Foggi, R. G. Brown *Chem. Phys. Lett.* **2000**, *319*, 157; b) R. de Vivie-Riedle, V. De Waele, L. Kurtz, E. Riedle *J. Phys. Chem. A* **2003**, *107*, 10591; c) S. Lochbrunner, K. Stock, E. Riedle, *J. Mol. Struct.* **2004**, *700,* 13; d) S. Lochbrunner, K. Stock, C. Schriever, E. Riedle in *Ultrafast Phenomena XIV* (Eds.: T. Kobayashi, T. Okada, T. Kobayashi, K. Nelson, S. De Silvestri), Springer, Berlin, **2005**, 491; e) S. Lochbrunner, C. Schriever, E. Riedle, In *Hydrogen-Transfer Reactions*, (Eds.: J. T. Hynes, J. P. Klinman, H.-H. Limbach, R. L. Schowen), Wiley-VCH, Weinheim, 2006, 349.

[15] V. Cañibana, J. F. Rodriguez, M. Santos, A. M. Sanz-Tejedor, M. C. Carreño G. Gonzalez, J. L Garcia-Ruano , *Synthesis*, **2001**, 2175.

[16] A. Burghart, H. Kim, M. B. Welch, L. H. Thoresen, J. Reibenspies, K. Burgess, *J. Org. Chem.*, **1999**, *64*, 7813–7819.

[17] L. H. Vogt Jr., J. G. Wirth *J. Am. Chem. Soc.* **1971**, *93*, 5402.

[18] a) N. Armaroli *Chem. Soc. Rev.* **2001**, *30*, 113; b) D. Felder, J. F. Nierengarten, F. Barigelletti, B. Ventura, N. Armaroli *J. Am. Chem. Soc.* **2001**, *123*, 6291; c) L. X. Chen, G. Jennings, T. Liu, D. J. Gosztola, J. P. Hessler, D. V. Scaltrito, G. J. Meyer *J. Am. Chem. Soc.* **2002**, *124*, 10861; d) Z. A. Siddique, Y. Yamamoto, T. Ohno, K. Nozaki *Inorg. Chem.* **2003**, *42*, 6366; e) N. Armaroli, G. Accorsi, F. Cardinali, A. Listorti *Top. Curr. Chem.* **2007**, *280*, 117.

[19] *Handbook of Photochemistry,* 3rd ed (Eds: M. Montalti, A. Credi, L. Prodi, M. T. Gandolfi), CRC Press, Boca Raton, 2006.

[20] M. Galletta, F. Puntoriero, S. Campagna, C. Chiorboli, M. Quesada, S. Goeb, R. Ziessel, *J. Phys. Chem. A.*, **2006**, *110*, 4348 and refs therein.

[21] Notably, the high-energy emission exhibited by **3** and **4** could not be necessary due to the Franck–Condon state, but could originate from an excited state in which some structural change is occurred but it is not the complete ESIPT process (for example, a single-proton transfer). At the moment, we have no way to explore this point in more detail. Most likely, theoretical investigations would be needed, but they are out of the scope of this paper.

[22] F. Loiseau, C. Di Pietro, S. Campagna, M. Cavazzini, G. Marzanni, S. Quici, *J. Mater. Chem.*, **2005**, *15*, 2762.

[23] a) G. A. Crosby, J. N. Demas, *J. Phys. Chem.* **1971**, *75*, 991; b) K. Nakamaru, *Bull. Chem. Soc. Jpn.* **1982**, *55*, 2697.

[24] Enraf-Nonius, Delft, The Netherlands, **1997**.

[25] Z. Otwinovski, W. Minor, *Macromolecular Crystallography*, Part A in *Methods in Enzymology*, Academic Press 1**997**, 307.

[26] A. Altomare, M. C. Burla, M. Camalli, G. L. Cascarano, C. Giacovazzo, A. Guagliardi, A. G. G. Moliterni, G. Polidori, R. Spagna, *J. Appl. Crystalogr.* **1999**, *32*, 115.

[27] J. G. Wirth *US Patent* **1973**, 3, 676.

[28] D. R. Coulson, *Inorg. Synth.* **1972**, *13*, 121.

[29] K. T. Potts, K. Dilip, *J. Org. Chem.* **1991**, *56*, 4815.

Received: November 16, 2007
Revised: January 17, 2008
Published online: March 25, 2008

  